A Frequency-optimized Discontinuous Formulation for Wave Propagation Problems

Yi Li[1] and Z. J. Wang[2]

Department of Aerospace Engineering and CFD Center, Iowa State University, Ames, IA 50011

Recently, a new unifying discontinuous formulation was developed by Huynh [7], and extended to simplex and hybrid meshes by Wang & Gao [21] for hyperbolic conservation laws. As with almost all discontinuous methods such as the discontinuous Galerkin, spectral volume and spectral difference methods, the new formulation named CPR (Correction Procedure via Reconstruction) employs a piece-wise discontinuous polynomial space. In this paper, a hybrid discontinuous space including polynomial and Fourier bases is employed in the CPR formulation to compute broad-band waves. The dispersion and dissipation properties of this method are investigated through a Fourier analysis. The analysis is also used to guide the selection of free-parameters to optimize the resolution of broadband waves and minimize both dissipation and dispersion errors. The results are verified with numerical solutions of the simple scalar advection equation and the two-dimensional acoustic wave equations.

Keywords: CPR (Correction Procedure via Reconstruction), A Hybrid Discontinuous Space, Wave Propagation Analysis

I.   Introduction

High-order methods are highly desired for wave propagation problems including aero-acoustic and electromagnetic waves. As pointed by Tam [13], aero-acoustic problems are intrinsically unsteady, and the dominant frequency is usually high. They differ from general computational fluid dynamics problems. Many powerful numerical algorithms have been developed to solve computational aeroacoustics (CAA) problems, e.g. the dispersion-relation-preserving (DRP) finite difference schemes [14], discontinuous Galerkin method [6], multi-domain spectral methods [3], spectral volume and difference methods [10, 19, 22], compact schemes [1, 4] and WENO schemes[2, 5, 20].

   High-order methods capable of handling unstructured grids are obviously much more flexible in dealing with complex geometries. In this paper, we focus on a recent discontinuous unstructured grid formulation called CPR (Correction Procedure via Reconstruction) [7, 21], which unifies the DG and SV/SD methods. In most discontinuous methods, local spaces based on polynomials are used. Non-polynomial bases have been studied in [23], and demonstrated for problems with special solutions. In the present study, we employ hybrid bases including both polynomials and Fourier bases to resolve broad-band wave propagation problems. We borrow the ideas from the DRP and upwind DRP schemes in determining the parameters in the Fourier bases to maximize the resolvable wave number given a certain error threshold. The basic idea of DRP scheme is to optimize the scheme coefficients for the high resolution of short waves with respect to the computational grid instead of the truncation error in [12, 14, 25, 26]. A suitable grid density can be determined by the grid requirement (points-per-wavelength, PPW) following the same procedure as presented in [8, 24] without boundary condition consideration.

   The dispersive and dissipative errors were investigated to analyze the wave propagation performance and such a method was used for finite difference and finite volume methods [9, 12, 14, 25, 26]. Van den Abeele [18] performed such an analysis for the 1D spectral volume method and Hu [6] applied it for the discontinuous Galerkin method. The CPR method based on hybrid bases is analyzed using a similar method.

   This paper is organized as follows. For the sake of completeness, first the CPR method is reviewed in section 2. One-dimensional wave propagation analysis is given in section 3. The hybrid bases are optimized by minimizing dispersion and dissipation integrated errors given certain wave numbers and at the same time satisfying a given resolution error threshold. Wave propagation properties are investigated by using Fourier analysis for the optimized

---

[1] Graduate Student, Department of Aerospace Engineering, yili@iastate.edu, AIAA Student Member
[2] Professor of Aerospace Engineering, 2271 Howe Hall, zjw@iastate.edu, Associate Fellow of AIAA

American Institute of Aeronautics and Astronautics

hybrid bases. Then the mesh resolution analysis is given to verify the optimization procedure. In section 4, numerical results are presented to demonstration the performance of the numerical method with hybrid bases. Concluding remarks are given in section 5.

II.   Review of the CPR Formulation

The CPR formulation was developed in [7] and [21]. The basic idea is reviewed here. The conservation equation is given as

$$\frac{\partial Q}{\partial t} + \nabla \cdot \vec{F}(Q) = 0 \tag{2.1}$$

where $\vec{F}$ is the flux vector. Multiplying (2.1) with an arbitrary weighting function W and integrating over an element V_i , we obtain

$$\int_{V_i} \left(\frac{\partial Q}{\partial t} + \nabla \cdot \vec{F}(Q) \right) W dV = \int_{V_i} \frac{\partial Q}{\partial t} W dV + \int_{\partial V_i} W \vec{F}(Q) \cdot \vec{n} ds - \int_{V_i} \nabla W \cdot \vec{F}(Q) dV = 0 \tag{2.2}$$

Let Q_i^h be an approximate solution to Q at element i. Because the approximate solution is discontinuous across the element interface, the face flux term is replaced with a common Riemann flux

$$\tilde{F}^n(Q_i^h, Q_{i+}^h, \vec{n}) \approx F^n(Q_i^h) = \vec{F}(Q_i^h) \cdot \vec{n} \tag{2.3}$$

where Q_{i+}^h is the solution outside the current element V_i. Equation (2.2) then becomes

$$\int_{V_i} \frac{\partial Q_i^h}{\partial t} W dV + \int_{\partial V_i} W \tilde{F}^n(Q_i^h, Q_{i+}^h, \vec{n}) ds - \int_{V_i} \nabla W \cdot \vec{F}(Q_i^h) dV = 0 \tag{2.4}$$

Applying integration by parts to the last term, we obtain

$$\int_{V_i} \frac{\partial Q_i^h}{\partial t} W dV + \int_{V_i} W \nabla \cdot \vec{F}(Q_i^h) dV + \int_{\partial V_i} W [\tilde{F}^n(Q_i^h, Q_{i+}^h, \vec{n}) - F^n(Q_i^h)] ds = 0 \tag{2.5}$$

The term $[\tilde{F}] = \tilde{F}^n(Q_i^h, Q_{i+}^h, \vec{n}) - F^n(Q_i^h)$ is the normal flux difference and can be viewed as a penalty term. A correction field δ_i is introduced using the following lifting operator, which is defined as

$$\int_{V_i} W \delta_i dV = \int_{\partial V_i} W [\tilde{F}] ds. \tag{2.6}$$

We obtain

$$\int_{V_i} \left[\frac{\partial Q_i^h}{\partial t} + \nabla \cdot \vec{F}(Q_i^h) + \delta_i^h \right] W dV = 0 \tag{2.7}$$

Under some mild conditions outlined in [21], (2.7) can be reduced to a differential form. Let the degrees of freedom (DOFs) be the solutions at solution points (SPs) and the equation (2.7) is the true at the SPs, i.e.,

$$\frac{\partial Q_{i,j}^h}{\partial t} + \nabla \cdot \vec{F}(Q_{i,j}^h) + \delta_{i,j}^h = 0 \tag{2.8}$$

Equation (2.8) does not involve any explicit surface or volume integrals, and the lifting operator depends on the choice of weighting function W. The performance of this formulation depends on how efficiently the correction field δ can be computed.

III.   One-Dimensional Wave Propagation Analysis

A. Introduction to wave Propagation Analysis

The dispersive and dissipative properties of the spatial discretization of the CPR method will be analyzed. The approach is following the methods by Hu [6] and Van den Abeele [18]. In this section, 1D CPR will be analyzed.

The 1D scalar advection equation with periodic boundary conditions and a harmonic wave as the initial solution is given as

$$\frac{\partial u}{\partial t} + a \frac{\partial u}{\partial x} = 0 \tag{3.1}$$

$$u(x, 0) = e^{ikx} \tag{3.2}$$

\hwhere a is the positive wave speed. The dispersion of the scheme $u(x,t) = \hat{u}e^{I(kx-\omega t)}$ represents a sinusoidal wave train with a wave number k and a frequency ω. The exact dispersion relation for (3.1) is $\omega = ak$. To (3.1), a (p+1) degree of freedom (DOF) method will be applied on a uniform mesh of size Δx. On a local coordinate $\xi \in [-1, 1]$ for each element i, the approximation $u_i = \sum_{j=1}^{P+1} u_{i,j} L_j$ can be written as a function of ξ. On the boundaries between two elements, a Riemann flux is used

$$F^R\big(u_i(1), u_{i+1}(-1)\big) = a\left(\tfrac{1+a}{2}u_i(1) + \tfrac{1-a}{2}u_{i+1}(-1)\right) \tag{3.3}$$

In (3.3), $\alpha = 0$ corresponds to a central flux and $\alpha = 1$ corresponds to the upwind flux. Upwind flux is used here. Equation (3.1) then becomes

$$\sum_{j=1}^{p+1} \delta_{mj}\frac{du_{i,j}}{dt} + \sum_{j=1}^{p+1} N_{mj}^{-1} u_{i-1,j} + \sum_{j=1}^{p+1} N_{mj}^0 u_{i,j} = 0, \quad m = 1, \dots, p+1 \tag{3.4}$$

The matrix elements N_{mj}^{-1} and N_{mj}^0 are given by the following expressions:

$$N_{mj}^{-1} = -2 * \frac{L_m(-1)L_j(1)}{M^{-1}} \qquad m, j = 1, \dots, p+1 \tag{3.5}$$

$$N_{mj}^0 = 2 * \frac{\partial L_j(\xi)}{\partial \xi}(\xi_m) + 2 * \frac{L_m(-1)L_j(-1)}{M^{-1}} \qquad m, j = 1, \dots, p+1 \tag{3.6}$$

M^{-1} is the inversion matrix of M, and $M_{mj} = \int_{-1}^{1} L_m(\xi) L_j(\xi)d\xi$ ($m, j = 1, \cdots, p+1$). The non-dimensional wave number and frequency are defined as $K = k\Delta x$ and $\Omega = \omega\Delta x/a$, and the exact dispersion relation is given as $\Omega = K$. Substituting the expression of a harmonic wave $u(x,t) = \hat{u}e^{I(kx-\omega t)}$ into (3.1), the numerical dispersion relation determined for upwind flux is given as

$$det\big(-I\Omega + e^{-IK}N^{-1} + N^0\big) = 0 \tag{3.7}$$

The quantity $-I\Omega$ is called the Fourier footprint $\mathfrak{R}$ and $\mathfrak{R} = \mathfrak{R}^{Re} + i\mathfrak{R}^{Im}$, and the imaginary part $\mathfrak{R}^{Im}$ is a measure of dispersive properties of the scheme, whereas the real part $\mathfrak{R}^{Re}$ represents the diffusive behavior which should be non-positive to keep the scheme stable. For classic finite difference methods with one DOF, the wave range is $-\pi < K < \pi$, while with p+1 DOF per cell, the wave range is $-(P+1)\pi < K < (P+1)\pi$.

B. Hybrid Bases and Optimization of Free-Parameters

The piecewise polynomial bases are generally used as local spaces in most discontinuous methods. Non-polynomial approximation bases such as exponential functions and trigonometric functions for the discontinuous Galerkin (DG) method were developed in [23] to obtain better approximation for specific types of PDEs and initial and boundary conditions. The upwind CPR method based on hybrid bases is studied, with objective of resolving broad-band wave propagation problems. Hybrid bases are given as

$$T \in span(1, x, x^2, x^3, \cdots, \sin(\alpha 1 * x), \cos(\alpha 1 * x), \sin(\alpha 2 * x), \cos(\alpha 2 * x), \cdots) \tag{3.8}$$

where $(\alpha 1, \alpha 2, \alpha 3 \cdots)$ are free-parameters.

Acoustic problems are governed by the same equations as those in aerodynamics such as the Euler and Navier-Stokes equations. However minimum numerical dispersions and dissipations are required to get an accurate amplitude and phase for numerical calculation of wave propagation [13]. The optimized schemes such as central DRP [14] and upwind DRP [25, 26] schemes are to assure the transform of the scheme be a good approximation of that the partial derivative over a certain range of wave number. The approximation of the first-order spatial derivative $\partial u/\partial x$ on uniform grids for a finite difference method is given by

$$\left(\frac{\partial u}{\partial x}\right)_i \approx \frac{1}{\Delta x}\sum_{j=-N}^{M} a_j u(x_i + j\Delta x) \tag{3.9}$$

The basic idea of DRP is that the coefficients are determined by requiring the Fourier transform of the finite difference scheme on the right of (3.9) to be a close approximation of the partial derivative on the left.

Free-parameters in the hybrid bases for the CPR method are optimized by mimicking the similar idea of DRP [14, 25] to maximize the resolvable wave number given a certain error threshold. The following two conditions are applied.
- The optimization process has to allow the normalized value of $\Omega_{Im}/N - K/N$ and Ω_{Re}/N to be as close to zero as possible for certain integration wave numbers.

$$E = \int_0^e |\Omega_{Im}/N - K/N|^2 dK + \lambda \int_0^e |\Omega_{Re}/N|^2 dK \qquad (3.10)$$

The weight λ is set as 0.2 to balance the L_2 norm of the truncated errors of dispersion and dissipation. And e is a predetermined optimized range of wave numbers.

- In order to quantify the resolution of the scheme, set the dispersion and dissipation errors to less than 0.5%, i.e.[6]

$$|\Omega_{Im} - K| < 0.005 \ and \ |\Omega_{Re}| < 0.005 \qquad (3.11)$$

Different free-parameters α are found to minimize the integration error E through numerical searches for a certain wave number integration range e with $T = (1, x, \sin(\alpha * x), \cos(\alpha * x))$ in Table 1. And the maximum resolvable non-dimensional wave number K_c are determined using (3.11) for each α with respect to a certain integration wave number in Table 2. K_c increases and then decreases with respect to α which is related to a certain integration range.

Table 1 Optimization free-parameter α of Fourier bases for $T = (1, x, \sin(\alpha * x), \cos(\alpha * x))$

Integration range (e)	α	E - Dispersion	E-diffusion	E
π (3.14)	1.4	2.1477e-09	2.7483e-08	7.6444e-09
5*π/4 (3.93)	1.7	1.6503e-07	1.0139e-06	3.6781e-07
3*π/2 (4.71)	2.1	3.8702e-06	2.4832e-05	8.8367e-06
7*π/4 (5.50)	2.4	6.1540e-05	2.6556e-04	1.1465e-04
2*π (6.28)	2.7	6.5403e-04	2.1424e-03	1.0825e-03

Table 2 Maximum resolvable wave number K_c for $T = (1, x, \sin(\alpha * x), \cos(\alpha * x))$

Integration range	α	K_c
π (3.14)	1.4	3.9336
5*π/4 (3.93)	1.7	4.2336
3*π/2 (4.71)	2.1	4.8336
7*π/4 (5.50)	2.4	2.0336
2*π(6.28)	2.7	1.6336

$\alpha = 2.1$ is referred as the optimized free-parameter, which minimizes the integration error E over a relatively large wave number integration range 4.71 with the dispersion and dissipation errors to less than 0.5% in equation (3.11). The same procedure is applied for the higher DOF scheme. $\alpha = 4.0$ is the optimized free-parameter with the integration wave number range 8.6 for $T = (1, x, x^2, x^3, \sin(\alpha * x), \cos(\alpha * x))$, and $\alpha1 = 4.5$ and $\alpha2 = 3.0$ are the optimized free-parameters with the integration wave number 9.42 for $T = (1, x, \sin(\alpha1 * x), \cos(\alpha1 * x), \sin(\alpha2 * x), \cos(\alpha2 * x))$.

In Fig 1, the upwind CPR scheme with optimized base $T = (1, x, \sin(2.1 * x), \cos(2.1 * x))$ is compared with polynomial space, Tam & Webb's central DRP and Zhuang & Chen's upwind DRP. This optimization scheme has less dispersion errors than the polynomial space and the Tam & Webb's central DRP scheme, but a little larger dispersion errors than Zhuang & Chen's upwind DRP scheme. It is able to resolve the waves with non-dimensional wave numbers as high as about 1.3 which is very close to the seven stencil scheme, although it is a four stencil scheme.
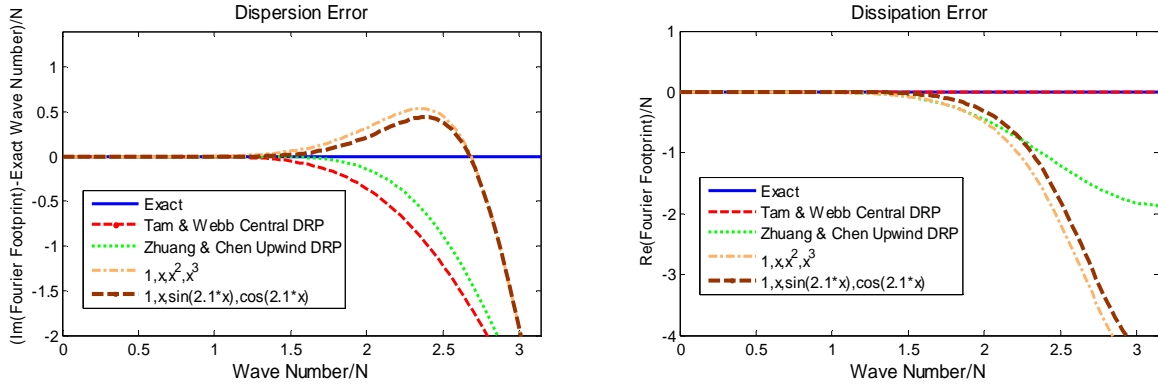
Fig.1. Comparison of dispersion errors $(\Omega_{Im} - K)/N$ and dissipation errors Ω_{Re}/N

C. Mesh Resolution Analysis

In this section, the mesh resolution analysis is applied to verify the optimization procedure by following the ideas in [8, 24]. The number of grid points per wavelength (PPW) is presented, with the objective of accurately simulating wave propagation over large distances. The mesh resolution analysis is based on the principle root $\sigma(K, C) = u_{m+1}/u_m$, where m is the current time step and m+1 is the next time step. K is the non-dimensional wave number, C is the courant number and PPW is the points per wave length and PPW $= \frac{\text{wavelength}}{\Delta x} = 2\pi/(k\Delta x)$. The local amplitude and phase errors are, respectively

$$\text{Error}_a = |\sigma| - 1 \tag{3.12}$$

$$\text{Error}_p = -\frac{\emptyset}{KC} - 1 \tag{3.13}$$

where $\emptyset = \tan^{-1}(\sigma_i/\sigma_r)$, and σ_i, σ_r are the real and imaginary part of σ, respectively. Criterion for comparing schemes is based on the global amplitude and phase errors which are

$$\text{Error}_a = \left| |\sigma|^{PPW*n/C} - 1 \right| < 10\% \tag{3.14}$$

$$\text{Error}_p = n * \left| \frac{PPW*\emptyset}{C} + 2\pi \right| < 10\% \tag{3.15}$$

where n is the number of the wavelength travelled. A very small courant number is used just for spatial consideration. This is a reasonable measure for selecting a grid density, and reveals the implications of optimization.
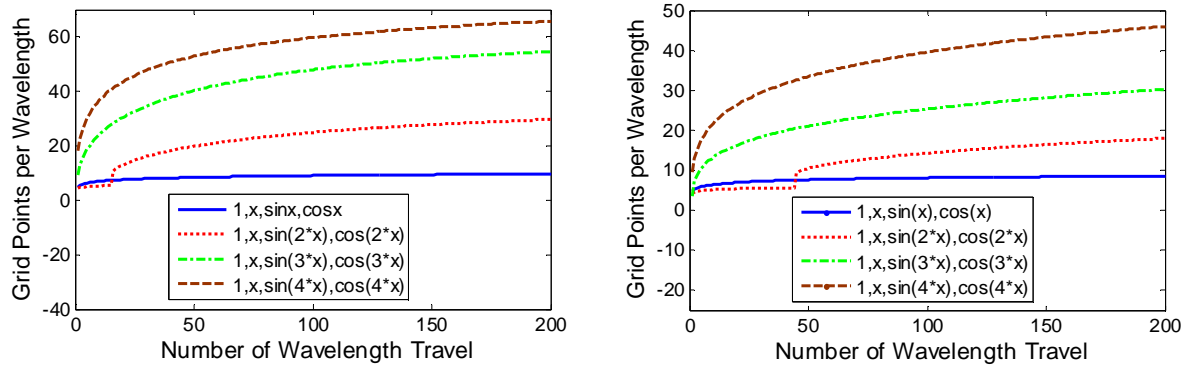

Fig.2. Grid resolution requirements based on globe amplitude and phase errors

In Fig 2, point per wavelength (PPW) requirement are presented for upwind CPR with respect to $\big(1, x, \sin(\alpha * x), \cos(\alpha * x)\big)$. $\alpha = 2$ is superior up to a distance of travel about 45 wavelengths based on 10% phase error

criterion. Such behavior is typical of optimized schemes. And usually aggressive optimization leads to excellent performance for small distances of travel but poor performance for longer distances. This property agrees with the previous analysis that the optimized free-parameter $\alpha = 2.1$, which is close to 2, shows good dispersive properties with the relatively large wave number given a certain resolution error criterion.

The PPW analysis matches the optimization analysis perfectly, and both methods can be used to verify each other. Because the schemes are optimized for a given range of wave number, they required fewer PPW if the propagation distance is relative short. As the number of wavelength traveled increase, the advantage of the optimized schemes diminished as the required PPW increase. However if fewer PPW is required, the use of optimized scheme not only gives most accurate results but also results in significant saving of CPU time.

IV. Numerical Tests

A. Exact Solution for 1D Wave Equation With Sine Wave as the Initial Condition

This problem is used to verify the performance of the wave propagation characteristics of CPR in terms of space $(1, x, sin(\alpha x), cos(\alpha x))$ and 1D convective wave equation is considered.

$$\frac{\partial u}{\partial t} + a\frac{\partial u}{\partial x} = 0 \ (a = 1) \tag{4.1}$$

On the uniform mesh with the initial condition is given as follows

$$u(x, 0) = sin(\pi x) \tag{4.2}$$

Due to Fourier spaces, the exact dispersion relation $\Omega = K$ is exactly satisfied at a certain K. For example if the base $T = (1, x, sin(2 * x), cos(2 * x))$ is applied, the physical value $\Omega = K = k * \Delta\xi = 2 * 2 = 4$. An approximation apace $(1, x, sin(\alpha x), cos(\alpha x))$ is designed to exactly simulate the equation.

- First set cell size Δx and calculate the initial condition's non-dimensional wave number $K_1 = k * \Delta x = \pi * \Delta x \ (k = \pi)$.
- Second choose a space $(1, x, sin(\alpha x), cos(\alpha x))$ and here $K_2 = \alpha * \Delta\xi \ (\Delta\xi = 2)$.
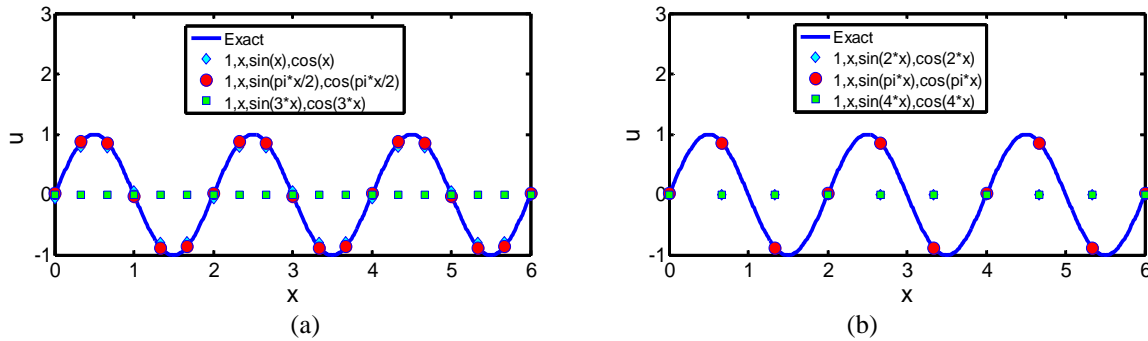- Finally set $K_1 = k_2 \xrightarrow{\text{yields}} \alpha = (\pi * \Delta x)/2$.

| (a) | (b) |

Fig 3. (a) $\alpha = (\pi * \Delta x)/\Delta\xi = \frac{\pi}{2}, \Delta x = 1, \Delta t = 0.01, T = 60$ (b) $\alpha = (\pi * \Delta x)/\Delta\xi = \pi, \ \Delta x = 2, \Delta t = 0.01, T = 60$

Fig 3 shows that the designed spaces exactly numerically simulate the wave equations (4.1) with the initial condition (4.2). (a) The space $(1, x, sin(\pi * x/2), cos(\pi * x/2))$ is exactly simulating the wave equation when $\Delta x = 1$ (b) The space $(1, x, sin(\pi * x), cos(\pi * x))$ is exactly simulating the wave equation when $\Delta x = 2$.

B. A Benchmark Problem – CAA Workshop (2004)

The governing equation is the scalar wave equation with unit wave speed as defined as equation (4.1), with the following initial condition

$$u(x, 0) = [2 + cos(\beta x)]exp[-ln2(x/10)^2], \ \beta = 1.7 \ or \ 4.6 \tag{4.3}$$

Two different frequencies $\beta = 1.7$ and $\beta = 4.6$ are considered, and set $\Delta x = 1$ for an equivalent 1 DOF. At this grid resolution, the high frequency wave embedded in the initial condition only has about 3.7 and 1.9 points-per-wave (PPW). It is therefore a challenge for any numerical scheme to adequately resolve the high frequency wave.
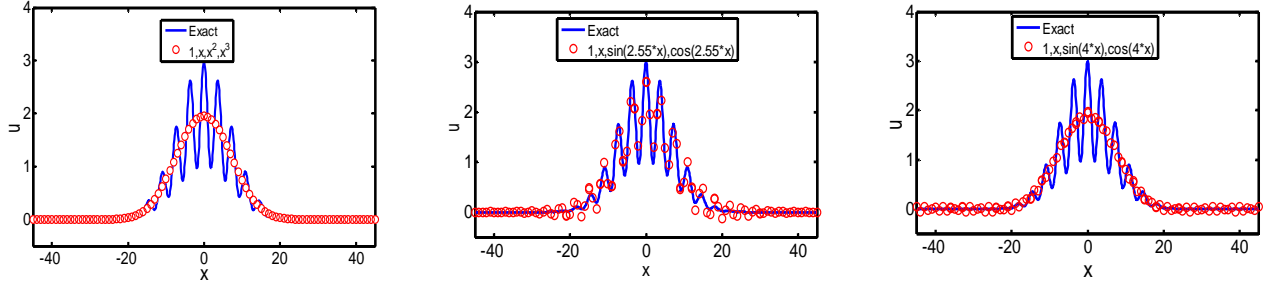
Fig 4. Numerical solution of 1D wave equation with the initial condition (5.3)
($T = 450s, \Delta x = 3$, 4th order DOF upwind scheme)

For $\beta = 1.7$, the approximation space $(1, x, \sin(\alpha x), \cos(\alpha x))$ is designed with $a = 2.55$ and $\Delta x = 3$ to exactly simulation the initial wave condition $\cos(\beta x)$. Then this approximation space is applied for the wave equation with the initial condition of equation (4.3) in order to get a better simulation. The time integration was carried out using a four-stage fourth-order Runge-Kutta scheme and a constant time step of 0.05s was used for all cases. In Fig 4, $a = 2.55$ shows much less dissipative behavior among the presented bases.
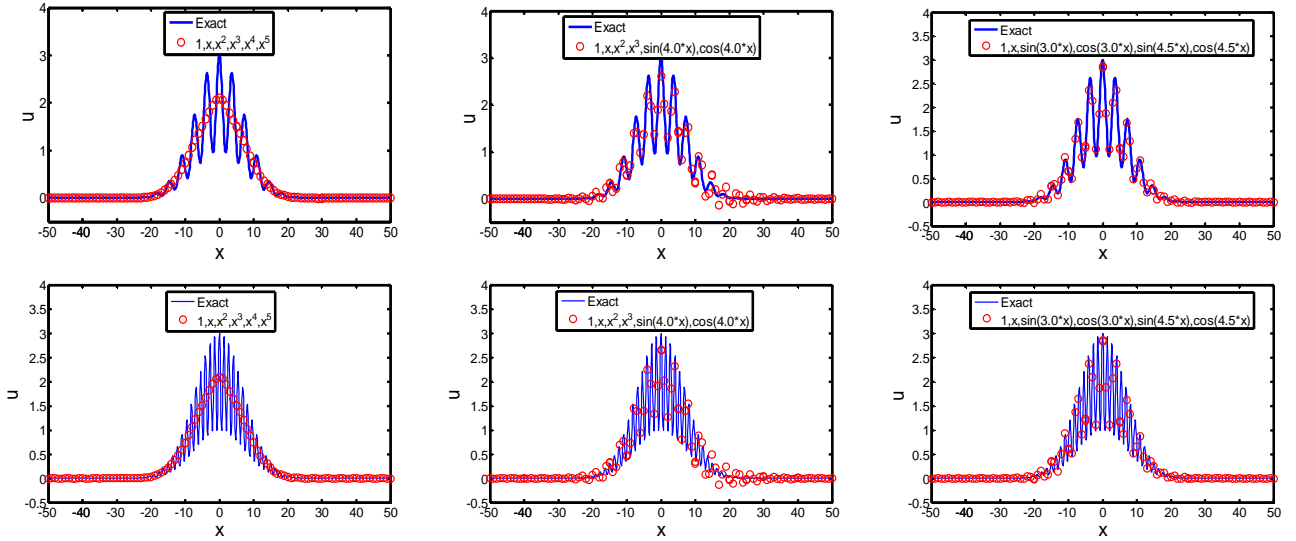

Fig 5. Numerical solution of 1D wave equation with the initial condition (5.3)
($T = 500$, $\Delta x = 5$, 6th order DOF upwind) and first row $\beta = 1.7$ and second row $\beta = 4.6$

In Fig 5, the solutions of CPR upwind scheme with the optimized approximation space $(1, x, x^2, x^3, \sin(4.0 * x), \cos(4.0 * x))$ and $(1, x, \sin(4.5 * x), \cos(4.5 * x), \sin(3.0 * x), \cos(3.0 * x))$ are compared with the 6th order polynomial approximation space for $\beta = 1.7 \ and \ 4.6$, and both schemes show better simulations than the polynomial approximation space. And the more Fourier bases terms there are, the more accurate the results are.

C. Two – Dimensional Acoustic Wave

This test case was computed for a 2D acoustic pulse. The governing equations for this test case are the 2D non-linear Euler equations

$$\frac{\partial Q}{\partial t} + \frac{\partial E}{\partial x} + \frac{\partial F}{\partial y} = 0 \tag{4.4}$$

where Q, E and F are vectors given by

$$Q = \begin{Bmatrix} \rho \\ \rho u \\ \rho v \\ \rho E \end{Bmatrix}, \quad E = \begin{Bmatrix} \rho u \\ \rho u^2 + p \\ \rho uv \\ u(\rho E + p) \end{Bmatrix}, \quad F = \begin{Bmatrix} \rho v \\ \rho uv \\ \rho v^2 + p \\ v(\rho E + p) \end{Bmatrix} \tag{4.5}$$

with ρ the mass density, u and v the velocity components and p the pressure. The total energy E is defined by the following equation

$$E = \frac{1}{\gamma-1}\frac{p}{\rho} + \frac{u^2+v^2}{2} \tag{4.6}$$

where γ is set to 1.4 which is the ratio of specific heat to air. The computations are carried out on three different structure grids (5x5), (10x10) and (20x20) on a square domain [0,1]x[0,1]. The initial solution is an acoustic pulse with a Gaussian profile and is set as same as one by Kris [15] [16]

$$\rho = \rho_\infty \left(1 + 0.001 * exp\left(-\frac{(x-0.5)^2+(y-0.5)^2}{r_0^2} \right) \right)$$
$$P = P_\infty + c_\infty^2(\rho - \rho_\infty) \tag{4.7}$$
$$u = 0$$
$$v = 0$$

And the ambient pressure, mass density and the half-width of the Gaussian profile are given as follows

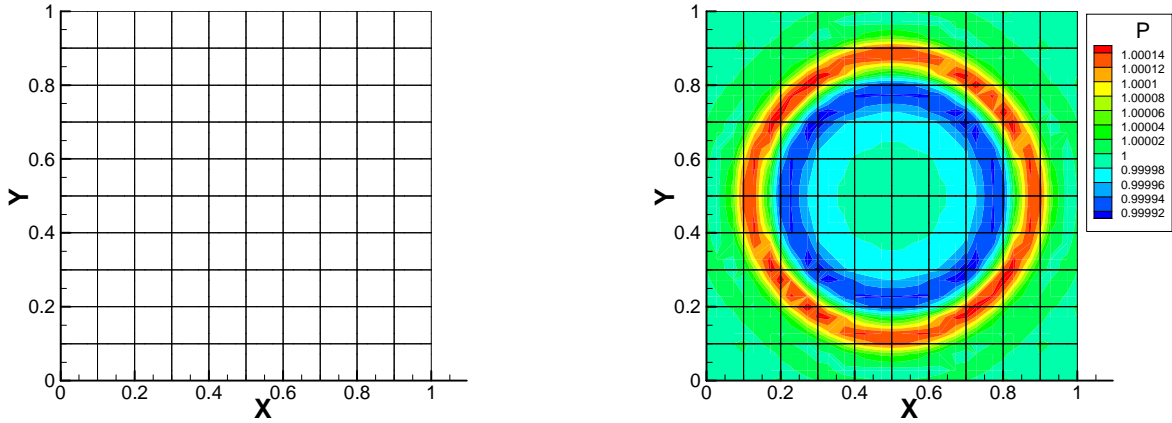$$P_\infty = 1, \quad \rho_\infty = 1, \quad r_0 = 0.05 \tag{4.8}$$

Fig 6. Structured quadrilateral 10x10 grids (left) and pressure contours (right) based on tensor product basis with approximation spaces $(1, x, x^2, x^3)$

The exact solution of the LEEs for the acoustic pressure field is given as

$$P_{ac}(t, x. y) = P - P_\infty = 0.001 * \frac{c_\infty^2 b^2}{2} \int_0^{+\infty} exp\left(-\left(\frac{\xi b}{2}\right)^2 \right) cos(\xi c_\infty t) J_0(\xi t)\xi d\xi \tag{4.9}$$

with $\eta = \sqrt{(x-0.5)^2 + (y-0.5)^2}$ and J_0 is the zero-th order Bessel function of the first kind which is used as a reference solution referring to [15] and [16].

Structured quadrilateral 10x10 grids are given on left of Fig 6 and pressure contours are given on the right of Fig 6 which is based on tensor product basis with approximation spaces $(1, x, x^2, x^3)$. Then the numerical schemes with 4th DOF optimized hybrid bases are tested. All numerical tests are carried out with $\Delta t = 0.0001s$, $T = 0.3s$, and Gauss-Lobatto points are used as distribution points for each element for CPR schemes.

In Fig 7, errors of the optimized bases $(1, x, sin(2 * x), cos(2 * x))$ are smallest among all of approximate bases shown for the 10x10 grids. This property agrees with the previous analysis that the optimized hybrid bases shows better dispersion and dissipation properties when non-dimensional wave numbers of the schemes are given in a certain range. In Fig 8 the optimized base still performs better than the corresponding polynomial base for the 20x20 grids. It is expected that the polynomial bases will perform best when the grids are fine enough.
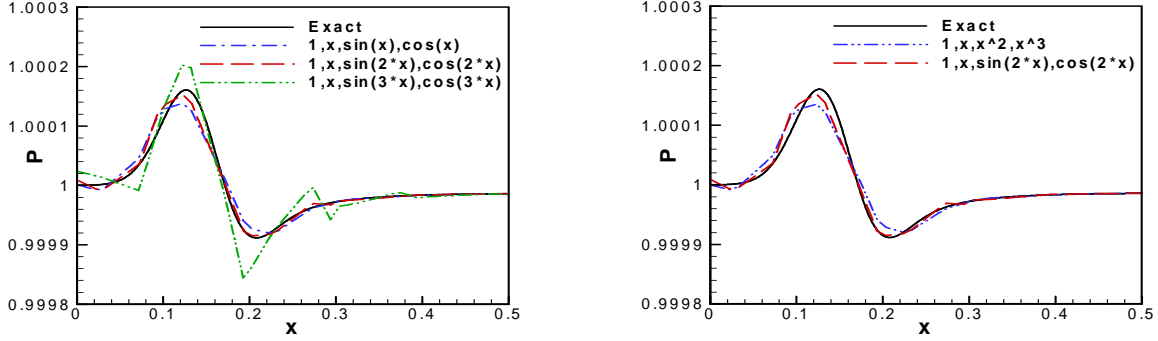
Fig 7. Pressure distribution at y = 0.5 (Tensor product bases with 4th order DOF) on 10x10 grids
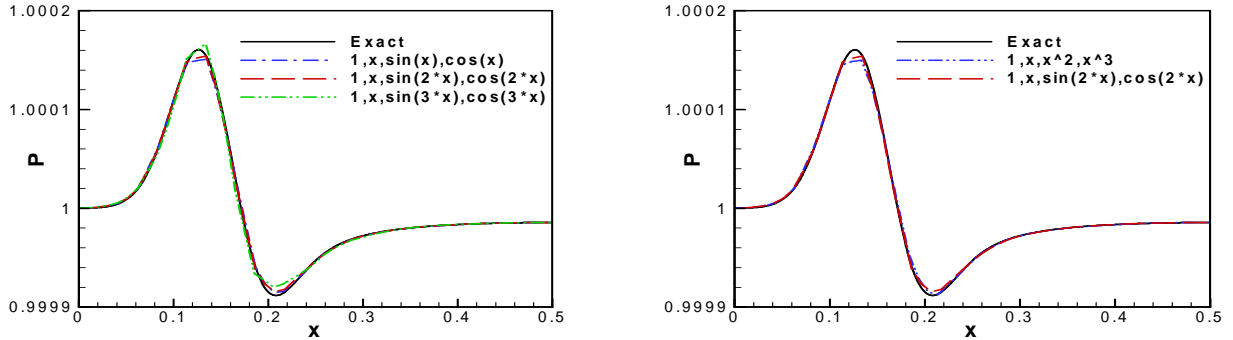

Fig 8. Pressure distribution at y = 0.5 (Tensor product bases with 4th order DOF) on 20x20 grids

V. Conclusion

The CPR (Correction Procedure via Reconstruction) formulation with a hybrid discontinuous space including polynomial and Fourier bases is studied. The free-parameters in the hybrid base are optimized based on minimizing both dispersion and dissipation errors and satisfying a certain resolution of dispersion and dissipation errors. The hybrid bases with optimized free-parameters show good wave propagation properties. A comparison was made with the dispersion and dissipation properties of the central DRP and upwind DRP schemes in 1D. The four-point stencil optimized hybrid bases is able to resolve waves with non-dimensional wave numbers as high as the seven-point stencil central and upwind schemes. And the more Fourier bases components are used, the less dispersion and dissipation errors the schemes show. Then the mesh resolution analysis is given to verify the optimized hybrid bases. The accuracy of the hybrid bases depends on the non-dimensional wave number.

Due to the Fourier bases included in the hybrid bases, the schemes can exactly simulate the wave equation at some specific non-dimensional wave number. This property is verified with the case with a sine wave as the initial condition. The method has been tested for Problem 1 in Category 1 (C1P1) on benchmark problem in the Fourth Computational Aeroacoustics (CAA) Workshop. It is shown that the scheme with optimized Fourier bases can resolve waves more accurately than the polynomial bases at 3.7 PPW. This is followed by the acoustic wave problem in 2D. It is verified again that the advantages of the optimized hybrid bases depend on the non-dimensional wave numbers.

References

[1]Graham Ashcroft and Xin Zhang, Optimized prefactored compact schemes, J. Comput. Phys. 190, pp. 459-477 (2003)

[2]D. Balsara And C. W. Shu, Monotonicity preserving weighted essentially non-oscillatory schemes with increasing high order of accuracy, J. Comput. Phys. 160, pp. 405-452 (2000)

[3]Bruno. Costa[a,] and Wai Sun Don[b], Multi-domain hybrid spectral-WENO methods for hyperbolic conservation laws , J. Comput. Phys. 224, pp. 970 – 991 (2007)

[4]R. Hixon, A new class of compact schemes, AIAA paper 98-0367, 1998

[5]Changqing Hu and Chiwang Shu, Weighted essentially Non-oscillatory schemes on Triangular meshes, J. Comput. Phys. 150, pp. 97-127 (1999)

[6]Fang Q. Hu, M. Y. Hussaini, Patrick Rasetarinera, An analysis of the discontinuous Galerkin method for wave propagation problems, J. Comput. Phys. 151, pp. 921-946 (1999)

[7] H.T. Huynh, A flux reconstruction approach to high-order schemes including discontinuous Galerkin methods, AIAA paper 2007-4079

[8]Henry Martin Jurgens, High-accuracy finite-difference schemes for linear wave propagation, Ph.D thesis, Department of Aerospace Science and Engineering, University of Toronto, 1997

[9]Yuguo Li, Wavenumber-Extended High-Order Upwind-Biased Finite-Difference Schemes for Convective Scalar Transport, J. Comput. Phys. 133, 235-255 (1997)

[10]Yen Liu, Marcel Vinokur, and Z.J.Wang, Discontinuous spectral difference methods for conservation laws on unstructured grids, in C. Groth and D.W. Zingg (Eds.), Proceeding of the 3rd international conference in CFD, Toronto, Springer, 2004, pp. 449-454

[11]Yen Liu, Marcel Vinokur, and Z.J.Wang, Spectral difference methods for unstructured grids I. Basic formulation, J. comput phys. 216, pp. 780-801 (2006)

[12]Hai-qing Si[a,*], Tong-guang Wang[b], Grid-optimized upwind dispersion-relation-preserving scheme on non-uniform Cartesian grids for computational aeroacoustics, Aerospace Science and Technology 12 (2008) 608-617

[13]C. K. W. Tam, Computational Aeroacoustics: Issues and Methods , AIAA Journal, Vol. 33, No. 10, 1995, pp. 1788-1796

[14]C. K. W. Tam and JAY C. WEBB, Dispersion-Relation-Preserving Finite Difference Schemes for Computational Acoustics, J. Comput. Phys. 107 (1993) 262-281

[15]Kris Van den Abeele, Development of high-order accurate schemes for unstructured grids, Ph.D thesis, Department of Mechanical Engineering, Vrije Universiteit Brussel, Belgium, (2008)

[16]Kris Van den Abeele [*,1], Chris Lacor, An accuracy and stability study of the 2D spectral volume method, J. Comput. Phys. 226, pp 1007-1026, (2007)

[17]Kris Van den Abeele, Chris Lacor, Z.J. Wang, on the connection between the spectral volume and the spectral difference method, J. Comput. Phys. 227 (2007) 877-885

[18]Kris Van Den Abeele, Tim Broeckhoven, Chris Lacor, Dispersion and dissipation properties of the 1D spectral volume method and application to a p-multigrid algorithm, J. Comput. Phys. 224 (2007) 616-636

[19]Z.J. Wang, Spectral (finite) volume method for conservation laws on unstructured grids: basic formulation, J. Comput. Phys. 178 (2002) 210–251

[20]Z.J. Wang* and R. F. Chen, Optimized Weighted Essentially Nonoscillatory Schemes for Linear Waves with Discontinuity, J. Comput. Phys. 174 (2001) 381-404

[21]Z.J. Wang* and Haiyang Gao, A Unifying Lifting Collocation Penalty Formulation including the discontinuous Galerkin, spectral volume/difference methods for conservation laws on mixed grids, Journal of Computational Physics 228 (2009) 8161-8186

[22]Z.J. Wang, Yen Liu, Spectral (finite) volume method for conservation laws on unstructured grids II: extension to two-dimensional scalar equation, J. Comput. Phys. 179, pp. 665 – 697 (2002)

[23]Ling Yuan, Chi-Wang Shu*, Discontinuous Galerkin method based on non-polynomial approximation spaces, J. Comput. Phys. 218 (2006) 295-323.

[24]D.W. Zingg, A review of high-order and optimized finite difference methods for simulating linear wave phenomena, AIAA Paper 97-2088.

[25]M. Zhuang* and R. F. Chen, Optimized Upwind Dispersion-Relation-Preserving Finite Difference Scheme for Computational Aeroacoustics, AIAA Journal. Vol. 36, No. 11, November 1998

[26]M. Zhuang and R.F.Chen, Application of high-order optimized upwind schemes for computational aeroacoustics, AIAA Journal, Vol. 40, No.3, March 2002.